JOURNAL OF GEOPHYSICAL RESEARCH, VOL. 92, NO. A3, PAGES 2555–2559, MARCH 1, 1987

An Analysis of the Shocklike Electrostatic Noise Observed During AMPTE Solar Wind Ion Releases

T. Z. MA AND D. A. GURNETT

Department of Physics and Astronomy, University of Iowa, Iowa City

N. OMIDI

Institute of Geophysics and Planetary Physics, University of California, Los Angeles

For the purpose of explaining the shocklike noise detected by the Ion Release Module (IRM) instruments during the Active Magnetospheric Particle Tracer Explorers (AMPTE) solar wind ion releases, we present an analysis of electrostatic waves produced by the interaction of the ion cloud with the solar wind. This analysis considers an arbitrary direction of propagation. It is found that in the absence of cold photoelectrons the maximum growth rate occurs almost perpendicular to the solar wind velocity. The wave growth is much higher than for propagation parallel to the solar wind direction, and is caused by an ion-ion interaction between the injected ions (Ba^+ or Li^+) and the solar wind protons. However, in the presence of cold photoelectrons, the growth rate for the ion-ion interaction is comparable or less than for parallel propagation, which is primarily an ion-electron interaction. Therefore both types of interactions are probably involved in generating the shock-like electrostatic noise. The ion-ion instability is more likely to occur in the later stage of the cloud expansion after the cold photoelectrons have escaped and the ion-electron instability is more likely, or at least comparable to the ion-ion instability, in the early stages when the photoelectrons are dominant.

1. INTRODUCTION

During the Active Magnetospheric Particle Tracer Explorers (AMPTE) solar wind lithium releases on September 11 and 20, 1984, and the barium releases on December 27, 1984, and July 18, 1985, intense bursts of electrostatic noise were observed on the upstream side of the ion cloud [*Gurnett et al.*, 1985, 1986*a*, *b*; *Häusler et al.*, 1986]. This noise was called shocklike electrostatic noise by *Gurnett et al.* [1986*a*] because of the similarity to noise observed in planetary bow shocks. The noise is believed to be generated by an interaction between the rapidly flowing solar wind protons and the ions produced by photoionizations of the gas cloud. A specific model for generation of the noise was analyzed by *Gurnett et al.* [1986*a*, *b*]. The parameters in this model are summarized in Table 1, some of which were measured quantities and others of which were assumed. Two groups of electrons were used: one relatively cold species representing the photoelectrons from the ionized gas cloud and the other relatively hot species representing electrons from the solar wind. The two groups of electrons were assumed to drift with the same velocity V_D in such a way that the total current is zero. All components were assumed to have a Maxwellian velocity distribution. The growth rate of waves propagating parallel to the solar wind velocity was shown to be in good qualitative agreement with the observations.

This paper represents an extension of the earlier analysis of *Gurnett et al.* [1986*a*, *b*] in that it considers an arbitrary angle of propagation relative to the solar wind direction. Since the largest wave intensities are expected to occur when the growth rate is highest, the objective is to find the direction of propagation that maximizes the growth rate. Both the lithium and barium releases are analyzed. Because the electron temperature was not measured, both cold and hot electron distributions are considered. As will be shown, if the electrons are relatively hot, as expected in the later stages of the cloud expansion, the largest growth rates occur at an oblique angle to the solar wind velocity. The instability in this case involves an ion-ion interaction. On the other hand, if the electrons are relatively cold, as expected in the early stages of the expansion, both the parallel propagating ion-electron instability and the obliquely propagating ion-ion instability have similar growth rates.

Paper number 6A8682.
0148-0227/87/006A-8682$02.00

2. ANALYSIS

Using the same model as that used by *Gurnett et al.* [1986*a*, *b*], the dispersion equation for electrostatic waves in a multicomponent Maxwellian plasma, ignoring the magnetic field, is given by

$$D(k, \omega) = 1 - \sum_j \frac{1}{2}\left(\frac{1}{k\lambda_{Dj}}\right)^2 Z'(\zeta_j) = 0 \tag{1}$$

where λ_{Dj} is the Debye length for the jth species, Z' is the derivative of the plasma dispersion function [see *Fried and Conte*, 1961] and

$$\zeta_j = \frac{\omega/k - V_j}{a_j} \tag{2}$$

where a_j is the thermal speed and ω is a complex number, whose real part is the frequency of the wave and imaginary part is the growth rate. If the growth rate is positive, the wave amplitude increases, and if it is negative, the wave amplitude decreases. The quantity $V_j = |\mathbf{V}_j| \cos \theta_j$ is the projection of the drift velocity of jth species onto the $\mathbf{k}$ direction and θ_j is the angle between $\mathbf{V}_j$ and $\mathbf{k}$. Equation (1) has been solved numerically using the parameters given by *Gurnett et al.* [1986*a*, *b*]

TABLE 1. Summary of Model Parameters

Quantities	Notations	Values
Lithium ion density	N_{Li^+}	variable
Lithium ion temperature	T_{Li^+}	2×10^3 °K
Barium ion density	N_{Ba^+}	variable
Barium ion temperature	T_{Ba^+}	2×10^3 °K
Solar wind proton density	N_p	8 cm^{-3}
Proton temperature	T_p	1×10^5 °K
Solar wind velocity	V_{sw}	460 km/s for lithium release 500 km/s for barium release
Hot electron density	N_e^h	variable
Hot electron temperature	T_e^h	5×10^5 °K
Cold electron density	N_e^c	variable
Cold electron temperature	T_e^c	5×10^4 °K
Electron drift velocity	V_D	variable

and listed in Table 1. The results are shown in Figure 1 for the lithium release and in Figure 2 for the barium release.

Figure 1 gives the maximum growth rate γ_{max} as a function of θ, the angle between $\mathbf{k}$ and the solar wind velocity $\mathbf{V}_{sw}$, for $T_{Li^+} = 2 \times 10^3$ °K, $T_e^h = 5 \times 10^5$ °K, $T_e^c = 5 \times 10^4$ °K, $T_p = 1 \times 10^5$ °K, $N_{Li^+} = N_p = 8$ cm^{-3}, and $V_{sw} = 460$ km/s. The maximum growth rate is the highest value of growth rate found by varying k. As can be seen, γ_{max} decreases as θ increases from 0° to about 70°, reaches a peak at about 80° and then falls rapidly as θ approaches 90°. Roughly the same dependence occurs both with (solid curve) and without (dashed curve) photoelectrons. Note that in the absence of photoelectrons ($N_e^c = 0$) the peak value of γ_{max} at $\theta = 82°$ is about 10 times higher than that at $\theta = 0°$. Therefore, for waves propagating at $\theta \simeq 82°$ the intensitities are expected to grow to much greater amplitude than for waves propagating at $\theta \simeq 0°$. However, in the presence of photoelectrons ($N_e^c = N_{Li^+}$) the peak value of γ_{max} at $\theta = 84°$ is almost the same as that at $\theta = 0°$. The growth rate at large angles is therefore quite sensitive to the photoelectron density. A similar dependence can also be seen for the barium case. Figure 2 shows a plot of γ_{max} versus θ for $T_{Ba^+} = 2 \times 10^3$ °K, $T_e^h = 5 \times 10^5$ °K, $T_e^c = 5 \times 10^4$ °K, $T_p = 1 \times 10^5$ °K, $N_{Ba^+} = 10N_p = 80$ cm^{-3}, and

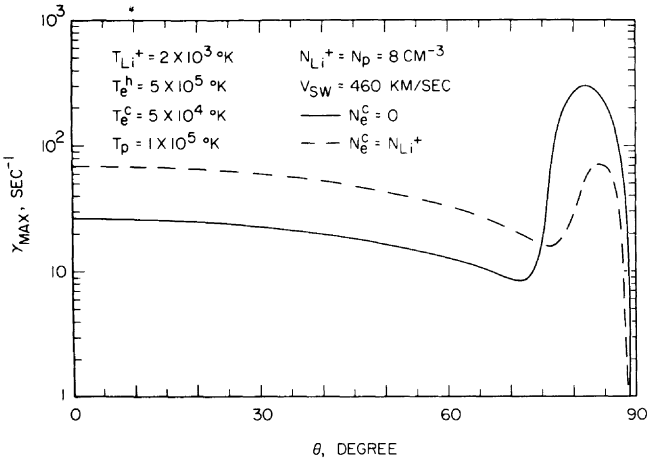

Fig. 1. The maximum growth rate γ_{max} (in s^{-1}) as a function of θ, the angle between $\mathbf{k}$ and $\mathbf{V}_{sw}$, for the case $T_{Li^+} = 2 \times 10^3$ °K, $T_e^h = 5 \times 10^5$ °K, $T_e^c = 5 \times 10^4$ °K, $T_p = 1 \times 10^5$ °K, $N_{Li^+} = N_p = 8$ cm^{-3}, and $V_{sw} = 460$ km/s. The solid curve is for $N_e^c = 0$, and the dashed curve is for $N_e^c = N_{Li^+}$.

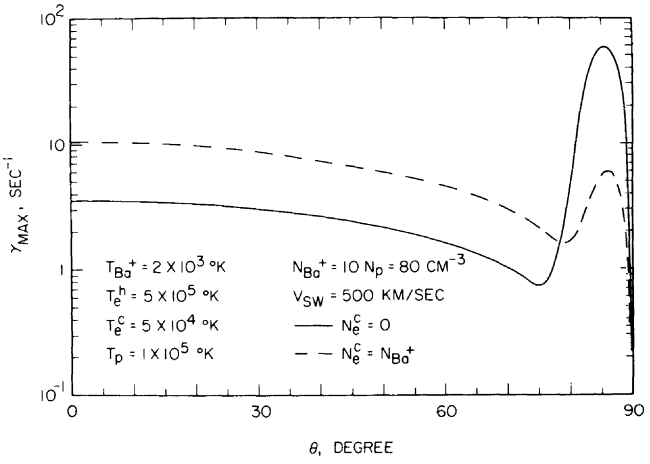

Fig. 2. The maximum growth rate γ_{max} (in s^{-1}) as a function of θ, for the case $T_{Ba^+} = 2 \times 10^3$ K, $T_e^h = 5 \times 10^5$ °K, $T_e^c = 5 \times 10^4$ °K, $N_{Ba^+} = 10N_p = 80$ cm^{-3}, and $V_{sw} = 500$ km/s. The solid curve is for $N_e^c = 0$, and the dashed curve is for $N_e^c = N_{Ba^+}$.

$V_{sw} = 500$ km/s. In the absence of photoelectrons (the solid curve) the peak growth rate at $\theta = 85.5°$ is more than 15 times the peak growth rate at $\theta = 0°$. However, in the presence of photoelectrons (the dashed curve) the peak growth rate at $\theta = 86°$ is less than the peak growth rate at $\theta = 0°$.

Further investigation shows that the frequency dependence of k and γ for large θ is very similar to that for $\theta = 0°$. Figure 3 shows this result. The top panel of Figure 3 shows the plot of the normalized wave number $k\lambda_D$, where λ_D is the Debye length, as a function of frequency, and the bottom panel shows the growth rate γ as a function of frequency. This plot is for the lithium case and uses $N_{Li^+} = N_p = 8$ cm^{-3}, $N_e^c = 0$, and $\theta = 82°$. This plot is almost the same as Figure 9 of *Gurnett et al.* [1986*a*], except the growth rate is much higher. The same results are also obtained for the barium case.

To study the dependence of the instability on the ion den-

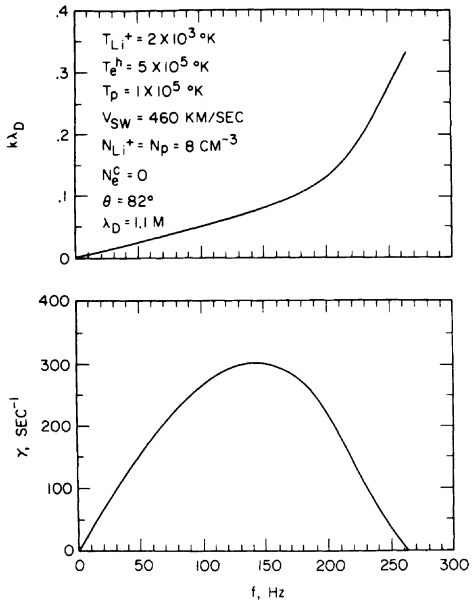

Fig. 3. A plot of $k\lambda_D$ versus frequency (top panel) and growth rate γ (in s^{-1}) versus frequency (bottom panel) for the lithium case, $T_{Li^+} = 2 \times 10^3$ °K, $T_e^h = 5 \times 10^5$ °K, $T_p = 1 \times 10^5$ °K, $V_{sw} = 460$ km/s, $N_{Li^+} = N_p = 8$ cm^{-3}, $N_e^c = 0$, and $\theta = 82°$.

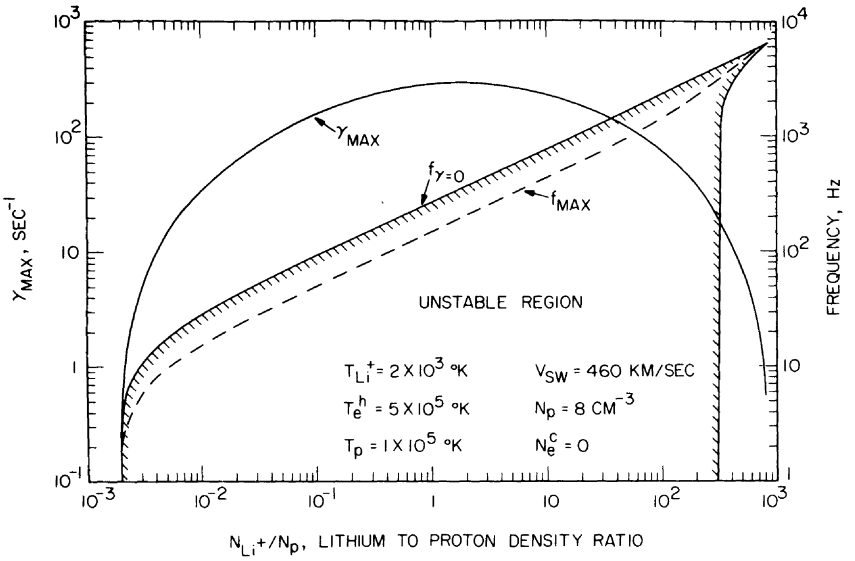

Fig. 4. A plot of maximum growth rate γ_{max} as a function of N_{Li}^+/N_p, the lithium to proton density ratio. The frequency for marginal instability, marked $f_{\gamma=0}$, is shown by the solid cross-hatched line, and the frequency associated with the maximum growth rate is shown by the dashed curve, marked f_{max}. These plots assume $T_{Li^+} = 2 \times 10^3$ °K, $T_e^h = 5 \times 10^5$ °K, $T_p = 1 \times 10^5$ °K, $V_{sw} = 460$ cm/s, $N_p = 8$ cm^{-3}, and $N_e^c = 0$.

sities, we calculate the maximum growth rate γ_{max} maximized over k and θ, and the frequency for the marginal instability ($\gamma = 0$), as a function of the density ratio N_{Li+}/N_p for the lithium case, and as a function N_{Ba+}/N_p for the barium case. Figures 4 and 5 show these results for the lithium case, and Figures 6 and 7 show the corresponding results for the barium case. In each figure the unstable region is the area under the marginal stability boundary $f_{\gamma=0}$. The dashed curve marked f_{max} is the frequency corresponding to the maximum rate γ_{max}. As can be seen by comparing Figure 4 with Figure 10 of *Gurnett et al.* [1986*a*], the unstable region for oblique propagation is much larger than for $\theta = 0°$. The instability occurs from $N_{Li}/N_p = 2 \times 10^{-3}$ to 8×10^2, and the unstable frequency range extends from 0 to about 6000 Hz. For $\theta = 0°$, instability occurs from $N_{Li+}/N_p = 0.02$ to 50 and the frequency range extends from 0 to 1500 Hz. The corresponding γ_{max} ranges up to 300 s^{-1}, about 10 times higher than for $\theta = 0°$. However, in the presence of cold photoelectrons (see Figure 5) the unstable region of N_{Li+}/N_p, the unstable frequency range, and the maximum growth rate γ_{max} are almost identical to those for $\theta = 0°$. A similar situation also occurs in the barium case. For the barium release, shown in Figure 6, in the absence of photoelectrons, it is seen that the unstable region for oblique propagation extends from $N_{Ba+}/N_p = 2 \times 10^{-3}$ to about 3×10^3, the unstable frequency range extends from 0 to about 3000 Hz, and γ_{max} extends up to 80 s^{-1}. However, in the presence of cold photoelectrons the unstable region is almost the same as that in the case $\theta = 0°$, and the growth rate γ_{max} is even less than that for $\theta = 0°$ [see *Gurnett et al.*, 1986*b*].

3. Discussion

As discussed by *Gurnett et al.* [1986*a*], for parallel propagation the instability is caused by an interaction between the

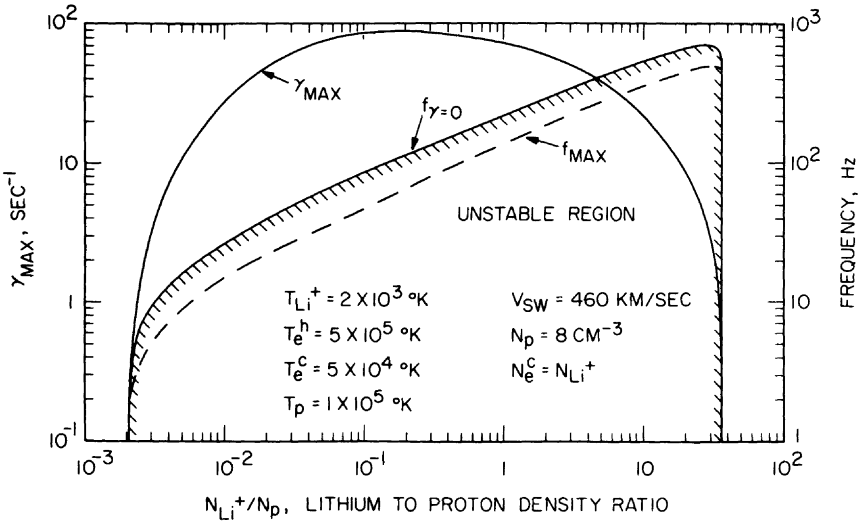

Fig. 5. The same plot as in Figure 4, for the case $T_e^c = 5 \times 10^4$ °K, $N_e^c = N_{Li^+}$.

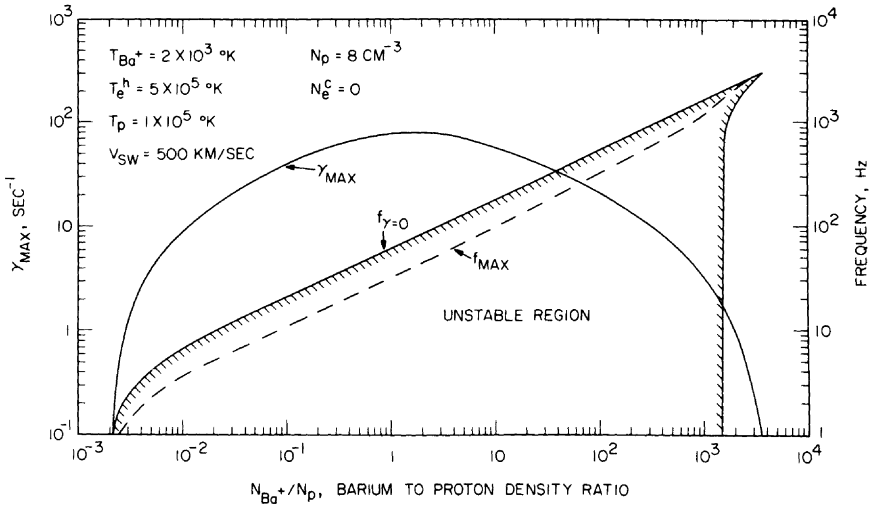

Fig. 6. The plot of γ_{max}, $f_{\gamma=0}$, f_{max} as marked in the figure as the functions of the barium to proton density ratio, N_{Ba^+}/N_p, for the case $T_{Ba^+} = 2 \times 10^3$ °K, $T_e^h = 5 \times 10^5$ °K, $T_p = 1 \times 10^5$ °K, $V_{sw} = 500$ km/s, $N_p = 8$ cm^{-3}, and $N_e^c = 0$.

injected ions and the electrons, very similar to a current-driven ion acoustic instability. This ion-electron instability tends to be most important when the electrons are cold because the slope of the electron distribution function increases as the electron temperature decreases. However, for oblique propagation, near 80°, the projected solar wind proton velocity becomes comparable to the ion acoustic speed, and the instability is caused by interaction between the solar wind proton beam and the injected ions. This ion-ion instability is most unstable when the electron distribution is very flat, i.e., when the electrons are very hot. If the electrons are cold, strong Landau damping tends to stabilize the ion-ion instability. The electron temperature therefore plays a very important role in controlling the two instabilities.

In conclusion, it appears that the shocklike noise observed upstream of the AMPTE solar wind ion releases can be generated by two instabilities. The first is an ion-electron instability that occurs for waves propagating parallel to the solar wind velocity. The second is an ion-ion instability that occurs for waves propagating at a large angle to the solar wind direction. Both instabilities give high growth rates for both the lithium releases and the barium releases. The calculated results agree with the observed results in all of the main features, such as the frequency range and the location where the noise occurs. At present, we are unable to determine which instability is actually dominant in any given case due to the lack of the information of the wave propagation direction and the temperature of the cold electrons. In the earlier stage of the ion cloud expansion, both instabilities are more likely to occur, and in the later stage of the expansion the ion-ion instability is more likely. This is because in the early stage the electrons are mostly from photoionization of the gas cloud and are probably very cold, $\sim 10^4$ °K, whereas in the later stages the photoelectrons have been replaced by much hotter, $\sim 10^5$ °K, solar wind electrons which enhance the ion-ion instability. Because of the very high growth rates, nonlinear effects are probably very important. Nonlinear interactions are expected to stabilize the system, to broaden the wave spectrum, and to saturate the growth rate. To understand fully the nonlinear processes involved, a numerical plasma simulation is necessary. These nonlinear effects will be explored in a separate paper.

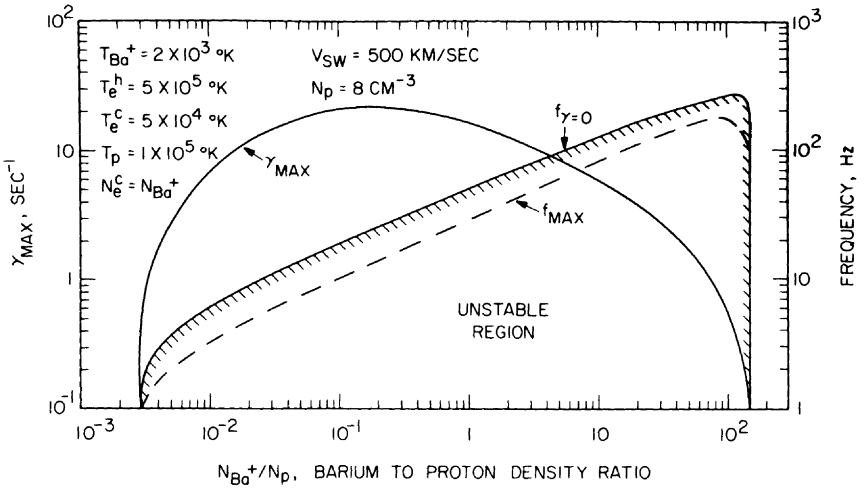

Fig. 7. The same plot as in Figure 6 for the case $T_e^c = 5 \times 10^4$ °K, $N_e^c = N_{Ba^+}$.

Acknowledgments. The research at the University of Iowa was supported by the Office of Naval Research through contracts N00014-82-K-0183 and N00014-85-K-0404 and by NASA through grants NGL-16-001-043 and NGL-16-001-002.

REFERENCES

Fried, B. D., and S. D. Conte, *The Plasma Dispersion Function*, Academic, Orlando, Fla., 1961.

Gurnett, D. A., R. R. Anderson, B. Häusler, G. Haerendel, O. H. Bauer, R. A. Treumann, H. C. Koons, R. H. Holzworth, and H. Lühr, Plasma waves associated with the AMPTE artificial comet, *Geophys. Res. Lett.*, *12*, 851, 1985.

Gurnett, D. A., T. Z. Ma, R. R. Anderson, O. H. Bauer, G. Haerendel, B. Häusler, G. Paschmann, R. A. Treumann, H. C. Koons, R. Holzworth, and H. Lühr, Analysis and interpretation of the shock-like electrostatic noise observed during the AMPTE solar wind lithium releases, *J. Geophys. Res.*, *91*, 1301, 1986*a*.

Gurnett, D. A., R. R. Anderson, T. Z. Ma, G. Haerendel, G. Paschmann, O. H. Bauer, R. A. Treumann, H. C. Koons, R. H. Holzworth, and H. Lühr, Waves and electric fields associated with the first AMPTE artificial comet, *J. Geophys. Res.*, *91*, 10,013, 1986*b*.

Häusler, B., L. J. Woolliscroft, R. R. Anderson, D. A. Gurnett, R. R. Holzworth, H. C. Koons, O. H. Bauer, G. Haerendel, R. A. Treumann, P. J. Christiansen, A. G. Darbyshire, M. P. Gough, S. R. Jones, A. J. Norris, H. Lühr, and N. Klöcker, Plasma waves observed by the IRM and UKS spacecraft during the AMPTE solar wind lithium releases: Overview, *J. Geophys. Res.*, *91*, 1283, 1986.

D. A. Gurnett and T. Z. Ma, Department of Physics and Astronomy, G483, University of Iowa, Iowa City, IA 52242.

N. Omidi, Institute of Geophysics and Planetary Physics, University of Southern California, Los Angeles, CA 90024.

(Received August 5, 1986;
revised November 14, 1986;
accepted October 23, 1986.)